Research on the deformation characteristics of small module tooth during current-assisted splitting spinning of small module tooth-shaped part

Haoyang Zhou[1], *Qinxiang* Xia[1*], *Chengxiu* Quan[2], and *Gangfeng* Xiao[1]

[1]School of Mechanical and Automotive Engineering, South China University of Technology, Guangzhou, 510641, China
[2]Department of Aircraft Maintenance Engineering, Guangzhou Civil Aviation College, Guangzhou 510403, China

Abstract. Aiming at the problems such as low material utilization, poor strength and toughness of workpiece during manufacturing of small module tooth-shaped parts (SMTSPs) by traditional gear hobbing and shaping method, a current-assisted splitting spinning forming (CASSF) method was proposed to form SMTSPs with high performance requirements. A coupled electrical-thermal-mechanical finite element (FE) model was established based on the ABAQUS software, and the distribution of equivalent stress and equivalent strain, and deformation characteristics of small module tooth were investigated. The results show that the equivalent stress and equivalent strain decrease from tooth groove arc to the tooth crest arc and centre of the tooth groove at tooth profile surface. The distribution of equivalent stress and equivalent strain in the internal deformation region follows the same trend as the tooth profile surface from the centre of the tooth groove to the tooth groove arc, but increases from the tooth groove arc to the tooth crest. The material of small module tooth experiences three-directional stress state. The material in the gear tooth undergoes radial and axial elongation, and tangential compression, while in the tooth groove it undergoes radial compression, tangential and axial elongation.
Keywords. Small module tooth-shaped parts, Current-assisted splitting spinning, Equivalent stress and strain, Deformation characteristics.

1 Introduction

Small module tooth-shaped parts (SMTSPs), as one of the most precise transmission components, are widely used in intelligent robots and high-end CNC machine tools due to their unique motion transmission and performance advantages [1]. Currently, gear hobbing and gear shaping are the mainstream manufacturing methods for SMTSPs. However, both hobbing and shaping involve material removal, leading to substantial material waste and environmental pollution. Additionally, the comprehensive mechanical properties of SMTSPs

* Corresponding author: meqxxia@scut.edu.cn

are weakened due to the interruption of metal fiber flow lines [2]. Therefore, it is imperative to develop a high-performance, efficient, and environmentally friendly manufacturing method for SMTSPs. Splitting spinning (SS) refers to a specific forming method by which the rotating circular blank being separated into "Y" shape gradually through the feeding of the splitting roller (SR) with sharp roundness radius [3]. Utilizing the electroplastic effect (EPE) in SS forming to reduce the deformation resistance of difficult-to-form metals and enhance plasticity is one of the most effective methods for achieving high precision requirements in SMTSPs forming.

In recent years, some scholars had investigated the deformation characteristics of materials during the current-assisted spinning forming process. Xu et al [4]. found that in the current-assisted deep drawing spinning process of cup-shaped parts, the bottom of the spun part is mainly affected by radial tensile strain and axial compressive strain, while the wall of the spun part is mainly affected by radial compressive strain and axial tensile strain. Li. et al. [5] an electric-thermal-mechanical coupled finite element model of current-assisted deep drawing spinning forming of cup-shaped part, and found that the equivalent strain of the spun part is uniformly distributed in the circumferential direction, and continuously increases along the axial direction from the bottom to the mouth, with the maximum value of equivalent strain appearing in the cup mouth. However, there is currently a lack of research on current-assisted splitting spinning (CASS) of differential, small module ($m<1$ mm), and high-tooth-count ($z \geq 100$) SMTSPs.

In this study, a coupled electric-thermal-mechanical FEA model for CASSF of SMTSP was developed based on the ABAQUS software, the distribution of equivalent stress and equivalent strain on small module tooth under the pulsed current, and the deformation characteristics of small module tooth were investigated.

2 Geometric model of SMTSP

The cup-shaped blank used in the CASSF is obtained through three-roller stagger spinning. The two-dimensional structure of the blank is shown in Fig. 1, and the material used is difficult-to-deform metal 30CrMnSiA alloy structural steel. The cup-shaped blank consists of a thick-walled region, a transition region, and a thin-walled region from the mouth to the bottom.

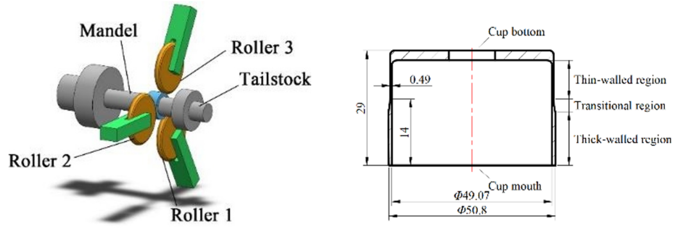

Fig. 1. Forming method for cup-shaped blank: (a) schematic illustration of the three-roller stagger spinning of cup-shaped blank (b) structure illustration of cup-shaped blank

2.1 Design method of Splitting roller tooth profile

During the CASSF process of the SMTP, the SR and the cup-shaped blank are subjected to pure rolling. According to the conjugate tooth profile principle, the tooth profile of the SR is the envelope curve generated by the tooth profile family of the SMTP at different positions during the meshing process. Fig. 2a shows the parameters of a specific tooth profile of the SMTP. Utilizing MATLAB simulation, the SR tooth profile is machined using the method of generating the envelope of the external teeth of the SMTP as a rotary roll. The envelope curves of the external teeth of the SMTP are plotted at various positions during the meshing process. Due to the excessive number of teeth on the SMTP, only two adjacent teeth are selected, and their envelope families during the meshing process are shown in Fig. 2b. The SR tooth profile is derived as shown in Fig. 2c.

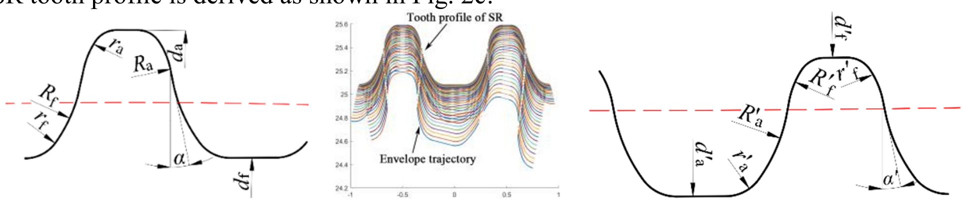

Fig. 2 Illustration of: (a) small module tooth (b) tooth envelope (c) splitting roller tooth

3 Establishment of FE Model for CASSF of SMTP

Both the electrical-thermal-mechanical solver based on the ABAQUS platform and the physical constitutive equations modified by Xia et al. [6] to account for the effects of pulsed current on 30CrMnSiA, have been employed to construct a local dimensions finite element analysis model for CASSF, as shown in Fig. 3. The SMTSP component features 160 teeth circumferentially and only the metal of transition region and thick-walled region underwent deformation during the actual forming process. A cup-shaped blank was truncated to 1/72 of the circumferential transition/thick-walled region to improve simulation efficiency. The simulation focused on the forming process of a single tooth. Baffles were added around the perimeter of 1/72 local dimensions model to constrain metal flow along the axial and circumferential directions. As the model has been simplified, the electrification method from the mouth of cup-shaped blank to the tailstock is equivalent to that from the lower conductive block to the mouth, then passing through the axial interface of the transition zone and the upper conductive block. Additionally, considering the thermal and electrical conduction between the upper/lower conductive blocks and the preform, the upper/lower conductive blocks were defined as deformable bodies.

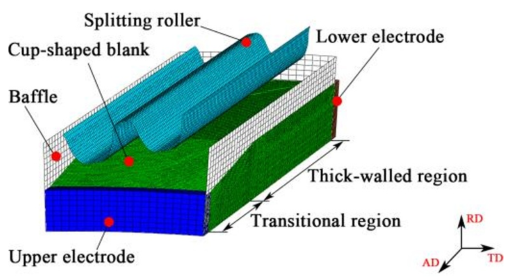

Fig. 3. Geometric model of CASSF of SMTSP

4 Results and Discussions

4.1 Equivalent stress distribution

Fig. 4 shows the distribution of equivalent stress in small module tooth during CASS with process parameters of the current density J_p = 9.5 A/mm^2, the duty ratio d = 70%, the rational speed of mandrel n_1 = 150 r/mm, the radial feeding velocity v_f = 0.01 mm/s, the reduction amount of material Δ = 0.2175 mm.

Different tooth positions are selected for analysis, where *a* and *b* represent the tooth profile surface and internal deformation region, respectively. Regions I, II, III, IV, and V respectively denote the tooth groove region of the leave-out side, tooth side wall of the leave-out side, tooth crest region, tooth side wall of the enter-in side, and tooth groove region of the enter-in side. The equivalent stress of the small module tooth is symmetrically distributed along the centerline of the tooth (subsequent analysis focuses solely on the distribution of equivalent stress and strain on the leave-out side).

As shown in Fig. 4, the equivalent stress gradually decreases from the tooth groove arc of region I to the tooth crest arc of region III, as well as to the center of region I. Additionally, the peak and valley values of the equivalent stress appear at the leave-out side of the tooth groove arc and the tooth crest circle, with values of 1180 MPa and 680 MPa, respectively. The distribution trend of the equivalent stress of curve *b* in regions I and II is consistent with that on the tooth profile surface. However, there is a gradual increase in stress from the region II to region III, and the peak value of the equivalent stress occurs in the tooth crest region. The reason is that the material in the middle of the gear tooth is squeezed by the material on both sides, and at the same time the material at the top of the tooth crest restricts the flow of the material in the middle of the tooth during the molding process. Therefore, the closer the material is to the center of the gear tooth, the greater the compressive stress it experiences.

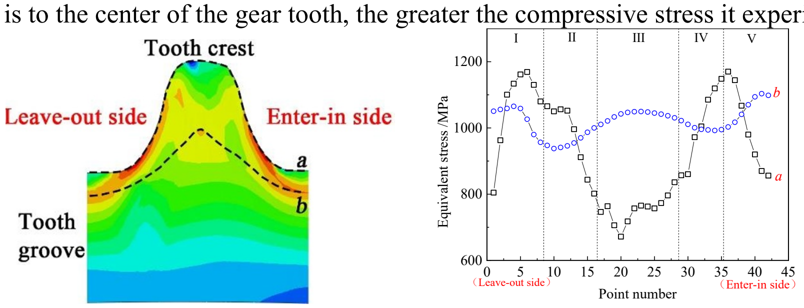

Fig. 4. shows the equivalent stress distribution of the tooth cross-section under J_p = 9.5 A/mm^2 d = 70%, n = 150 r/mm, v_f = 0.01 mm/s, Δ = 0.2175 mm

4.2 Equivalent strain distribution

Along the circumferential direction of the small module tooth, as depicted by curve *a* in Fig. 5, it is shows that the equivalent strain on curve *a* gradually increases from the center of the tooth groove and the tooth crest towards the tooth root arc. The maximum and minimum values of the equivalent strain occur respectively at the tooth root arc of the leave-out side and the region III. Moreover, the variation range of the equivalent strain on the tooth profile is remarkably pronounced.

The distribution trend of equivalent strain within the internal deformation region (curve *b*), is entirely opposite to curve *a*. The equivalent strain gradually increases from the tooth groove arc to the centre of the region I and region III. In the internal deformation region, the material deformation degree at the region III is greater than the region II. However, the variation range of the equivalent strain in deformation region significantly diminishes. Additionally, the lowest equivalent strain in small module tooth appears at the tooth crest and at the center of the tooth groove, indicating minimal plastic deformation in the material at the tooth crest and top of tooth groove. This suggests that the material in the tooth crest and top of tooth groove can be considered to undergo rigid translation motion during the CASS of SMTSP.

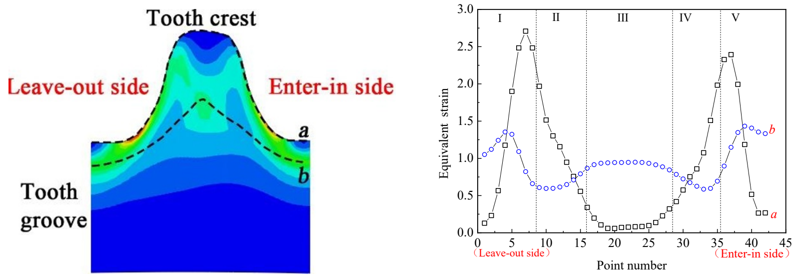

Fig. 5. shows the equivalent strain distribution of the tooth cross-section under J_p = 9.5 A/mm^2 d = 70%, n = 150 r/mm, v_f = 0.01 mm/s, Δ = 0.2175 mm

4.3 Deformation characteristics of small module tooth

The three-dimensional strain distribution of the material is shown in Fig. 6. In region C, the material undergoes radial compression deformation, while experiencing elongation deformations in the tangential and axial directions. In regions A and B, the material undergoes tangential compression deformation, accompanied by elongation deformations in the radial and axial directions. This phenomenon is attributed to the fact that in region C, the material experiences compression from the tooth of SR and is constrained by the mandrel, resulting in radial compression to form the tooth groove. Following the principle of constant plastic deformation volume, the material undergoes elongation in the tangential and axial directions. As for regions A and B, the material undergoes tangential deformation due to compression from the side of the SR side, while it remains unconstrained in the radial direction within the tooth groove of SR. Consequently, materials in regions A and B experience radial elongation, forming the gear teeth.

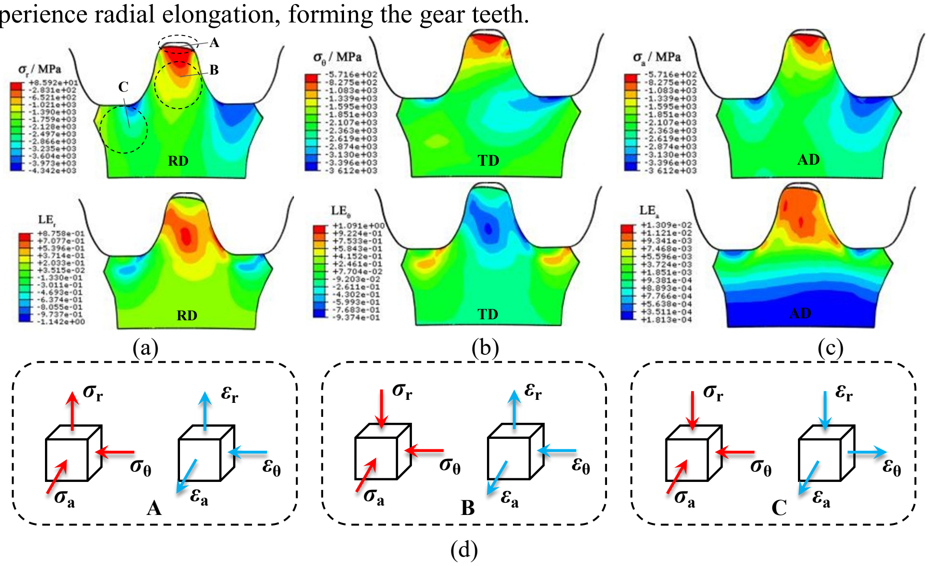

Fig. 6. Stress-strain distribution of small module tooth in different directions: (a) RD (b) TD (c) AD, and (d) states of stress and strain during the CASSF of SMTP ((RD, TD and AD denote the radial, tangential and axial direction, respectively; σ_r, σ_θ and σ_a denote the radial, tangential and axial stress, respectively; ε_r, ε_θ and ε_a denote the radial, tangential and axial strain, respectively.).

5 Conclusions

The tooth profile of the splitting roller is determined based on the principles of splitting spinning forming and the conjugate tooth profile engagement theory. The distribution of the equivalent stress and equivalent strain, and the deformation characteristics of small module tooth have been investigation based on FEA simulation.

1. The equivalent stress and strain on tooth profile surface gradually decreases from the tooth groove arc to the tooth crest arc, as well as to the center of tooth groove.

2. The distribution trend of the equivalent stress and strain on internal deformation region gradually decreases from the tooth groove arc to the center of tooth groove. However, there is a gradual increase from the tooth groove arc to tooth crest, and the peak value of the equivalent stress and strain occurs in the tooth crest region.

3. The material in the tooth groove and the middle of the gear tooth experiences three-directional compressive stress. The tooth crest is subjected to tensile stress in the radial direction and compressive stress in the tangential and axial directions. The tooth groove undergoes elongation deformation in the tangential direction and compression deformation in the radial and axial directions. Meanwhile, the tooth crest and the middle of the gear tooth experience elongation deformation in the radial direction and compression deformation in the tangential and axial directions.

Acknowledgement

This work was financially funded by the National Natural Science Foundation of China (No. 52175316), Guangdong Natural Science Foundation Project of Basic and Applied Basic Research (No. 2021A1515011074), and Guangzhou Science and Technology Planning Project (201804010135).

References

1. M. Kleiner, M. Geiger, A. Klaus, CIRP. Ann-Manuf. Techn., **52** (2003).
2. K. Gupta, R.F. Laubscher, J. Paulo, N.K. Jain, J. Clean. Prod. **112** (2016).
3. H. Li, R. Zeng, X. T. Zhang, J. J. Li, MATER DESIGN. **58**(2014).
4. Xu X, Wang L and Li Z Y (2020) Optimization on electrically assisted deep drawing spinning process for 30CrMnSiA cup-shaped part. *J. Forging & Stamping Technology* 45(01) pp 96-102. (in Chinese)
5. Li Z Y (2019). Research on electrically assisted deep drawing spinning method of cup-shaped blank used for flex spline. [Master's thesis, South China University of Technology]. Guangdong, China.
6. Q. X. Xia, C. Chen, G. F. Xiao, K. W. Chen, H. Y. Zhou, J. Mater. SCI, **58** (2023).